Amide Derivatives of DMABN: A New Class of Dual Fluorescent Compounds

D. Braun,[†] W. Rettig,*[,†] S. Delmond,[‡] J.-F. Létard,[‡] and R. Lapouyade[‡]

W. Nernst-Institut für Physikalische und Theoretische Chemie, Humboldt-Universität zu Berlin, Bunsenstrasse 1, D-10117 Berlin, Germany, and Laboratoire des Sciences Moleculaires, Institut de Chimie de la Matière Condensée de Bordeaux, Château de Brivazac, Avenue du Dr. Schweitzer, 33608 Pessac Cedex, France

Received: January 9, 1997; In Final Form: April 29, 1997[⊗]

Derivatives of DMABN are described, where the cyano group is replaced by an amide function with different acceptor strengths. This leads to a consistent variation of the dual fluorescence observed, describable within the established TICT model. Time resolved experiments give evidence of an additional complication with respect to DMABN due to the low-lying $n\pi^*$ state of the amides which induces a fluorescence quenching channel. The presence of various conformers leads to the observed nonexponential fluorescence decay traces.

1. Introduction

The dual fluorescence of *N*,*N*-dimethylaminobenzonitrile (DMABN) has been the subject of numerous investigations in the last decades, for reviews see refs 1−3. The TICT mechanism—"Twisted Intramolecular Charge Transfer"[1]—involving the torsional motion of the dimethylamino group in conjunction with electron transfer along the pathway of the adiabatic photoreaction channel has been widely used, but other mechanisms, such as a pyramidalization[4] or a Herzberg−Teller-coupling mechanism[5] as well as a mechanism involving solute−solvent exciplexes[6] have also been suggested. Common to all these mechanisms is the formation of two excited species: the primarily excited species, often called "locally excited" (LE) state emitting the short wavelength B-fluorescence band, and a secondary charge transfer (CT) species formed from the primary one, which emits the long wavelength A-fluorescence band.

In distinction to the other mechanisms, the TICT model has been very successful in predicting the ability of additional compounds to show dual fluorescence or in explaining why closely related compounds do not show dual fluorescence. Two factors are most important:[2] (i) sterical hindrance to planarity and (ii) increase of the donor−acceptor character favoring the formation of the TICT state. These factors can be used for predictions, and led to the discovery of dual fluorescence even in alkane solvents,[7,8] in the gas phase,[2] and under supersonic jet conditions.[9,10] Reducing the donor strength (less than two alkyl groups on the amino function) raises the energy of the TICT state and generally leads to the disappearance of the A-band, although sterical hindrance to planarity can induce it even for secondary amines.[11] Similarly, reduction of the acceptor strength should weaken the CT-band.

In this paper, we present a number of new DMABN derivatives bearing an amide acceptor function which allows the varying of the acceptor strength within the same substituent class. The dual fluorescence observed, as well as its solvent polarity dependence is fully consistent with the predictions from the TICT model, with the additional feature, revealed only by time-resolved measurements, of a quenching channel related to the $n\pi^*$ state.

The structure of the paper is as follows: the presentation of the experimental results is divided into two parts, starting with the simpler stationary measurements (absorption and fluorescence spectra and solvatochromic plots), and the time-resolved measurements including time-resolved fluorescence spectra as well as fluorescence decay traces analyzed by global analysis. In the discussion section, various conclusions are derived.

2. Experimental Section

2.1. Materials. 4-*N*,*N*-Dimethylaminobenzamide (DMABA) (formulas and abbreviations of the compounds used are listed in Figure 1) was obtained by isomerizing 4-*N*,*N*-dimethylaminobenzaldoxime with nickel acetate tetrahydrate as described by Field.[12] The product was subjected to silica-gel column chromatography and crystallized in ethanol, mp 209 °C (lit.[12] 208−209 °C).

4-*N*,*N*-Dimethylamino-*N*,*N*-dimethylbenzamide (DMABMA) was prepared by heating the acid chloride of 4-*N*,*N*-dimethylaminobenzoic acid and *N*,*N*-dimethylformamide at 150 °C for 4 h, according to the method of Coppinger.[13] The product crystallizes from ethanol, mp 95 °C (94−95 °C[13]). ^{1}H-NMR (250 MHz, $CDCl_3$) δ(ppm): 2.94 (6H, s), 3.02 (6H, s), 6.62 (2H, d, J = 8.8 Hz), 7.34 (2H, d, J = 8.8 Hz). ^{13}C-NMR (250 MHz, $CDCl_3$) δ(ppm): 40.23, 111.06, 123.05, 129.25, 151.29, 172.15. MS *m/z* (%, fragment): 192 (31, $M^{+\bullet}$), 148 (100, $-N(CH_3)_2$).

4-*N*,*N*-Dimethylamino-*N*,*N*-diethylbenzamide (DMABEA) was prepared from the acid chloride of 4-*N*,*N*-dimethylaminobenzoic acid and diethylamine. Crystallization from ethanol leads to white crystals, mp 72 °C. ^{1}H-NMR (250 MHz, $CDCl_3$) δ(ppm): 1.15 (6H, t, J = 7.1 Hz), 2.93 (6H, s), 3.40 (4H, q, J = 7.1), 6.63 (2H, d, J = 8.8 Hz), 7.28 (2H, d, J = 8.8 Hz). ^{13}C-NMR (250 MHz, $CDCl_3$) δ(ppm): 13.63, 40.28, 111.30, 124.36, 128.25, 151.06, 171.88. MS *m/z* (%, fragment): 220 (22, $M^{+\bullet}$), 148 (100, $-N(C_2H_5)_2$).

All solvents were of spectroscopic grade and tested for fluorescent impurities. Most of them were used without further purification; only glycerol triacetate (GTA) and butyronitrile were distilled several times under reduced pressure.

2.2. Measurements. The solutions were prepared to yield concentrations of 10^{-5}−10^{-4} mol/L. UV absorption spectra were recorded with a Cary 14 spectrometer. Corrected stationary fluorescence spectra were obtained on a Perkin Elmer 650-60 spectrofluorimeter. Fluorescence quantum yields were determined by comparison with quinine sulfate in 0.1 N sulfuric acid (Φ_f = 0.52).

[†] Humboldt-Universität zu Berlin.
[‡] Institut de Chimie de la Matière Condensée de Bordeaux.
[⊗] Abstract published in *Advance ACS Abstracts,* August 1, 1997.

S1089-5639(97)00168-0 CCC: $14.00

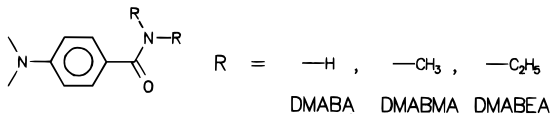

Figure 1. Formulas and abbreviations of the investigated compounds.

The fluorescence decay traces and time-resolved spectra at low temperatures were measured using a time correlated single-photon-counting setup and cooling equipment described previously.[14,15] Synchrotron radiation of the Berliner Elektronenspeicherring Gesellschaft für Synchrotron Strahlung mbH (BESSY), was the excitation light source which is characterized by a repetition rate of ~5 MHz and a full width at half-maximum (fwhm) of the excitation pulse of ~600 ps in the single-bunch mode. By setting polarizers at the magic angle, polarization effects were excluded. The fluorescence decay traces were analyzed by the iterative reconvolution technique[16] using the reduced χ^2 value ($\leq$1.2) as test for the quality of multiexponential fits, in terms of amplitudes α_i and time constants τ_i:

$$I_f = \sum_i \alpha_i \exp\left(-\frac{t}{\tau_i}\right) \quad (1)$$

The mean time constant $\langle\tau\rangle$ was calculated from the decay components τ_i according to

$$\langle\tau\rangle = \frac{\sum_i \alpha_i \tau_i}{\sum_i \alpha_i} \quad (2)$$

We used the program developed by Globals Unlimited for the global analysis, with simultaneous evaluation of several fluorescence decay traces at different wavelengths and reduction of the number of fitting parameters by linking the time constants within one set of experimental data.[17] Time-resolved spectra were measured by setting appropriate time windows using the time-to-amplitude converter and by scanning the wavelength.

3. Results

3.1. Stationary Experiments. Some interesting features can be observed in the absorption spectra presented in Figure 2. Isopentane as nonpolar and *n*-butyl chloride as medium polar solvents are compared. The absorption of the primary amide derivative DMABA is significantly shifted to longer wavelengths in contrast to the dialkyl amides DMABMA and DMABEA. The methyl- and ethyl-substituted compounds show a very similar absorption behavior. Two facts have to be emphasized: the distinctive shoulder around 300 nm in the low-energy part of the absorption spectra of DMABMA and DMABEA and the very broad maximum together with weaker longer wavelength shoulders in the DMABA spectra. On the basis of these experimental observations it can be suggested that the absorption spectra consist of two electronic transitions. The transition around 300 nm seems to be independent of the substituent on the amide function, whereas the higher energy transition shows a clear spectral blue shift for DMABMA and DMABEA. On the basis of comparison with other p-substituted donor-acceptor benzene derivatives,[1] we assign the shoulder to the ^1L_b-type and the stronger second band to the ^1L_a-type transition which shifts to the red when the acceptor strength is increased from DMABMA/DMABEA to DMABA. An increase of the solvent polarity induces the expected red shift of the ^1L_a-type band (Figure 2).

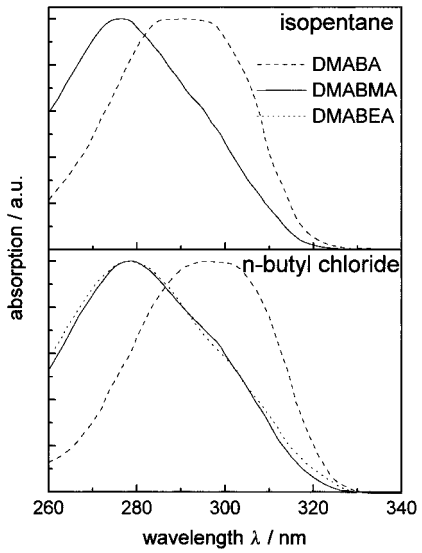

Figure 2. Normalized absorption spectra of DMABA, DMABMA, and DMABEA in isopentane and *n*-butyl chloride at room temperature.

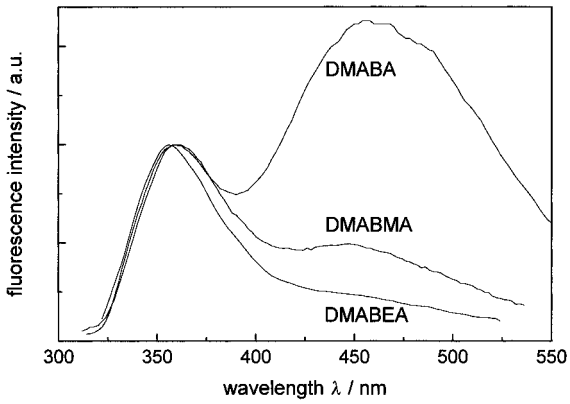

Figure 3. Corrected fluorescence spectra of DMABA, DMABMA, and DMABEA in *n*-butyronitrile at room temperature normalized to the short wavelength band maximum.

In the strongly polar solvent acetonitrile, the absorption spectra of the investigated compounds are consistent with Figure 2, lower part. For the absorption coefficient ϵ_{abs} of DMABMA, a value of 15500 L cm^{-1} mol^{-1} at λ_{max} = 280 nm was measured, for DMABEA 13800 l cm^{-1} mol^{-1} at λ_{max} = 276 nm. These ϵ-values are in the same range as for DMABN and its ester derivative.[18,19]

In Figure 3, the dual fluorescence of the three amide compounds in *n*-butyronitrile at room temperature are presented. The ratio of the fluorescence intensity of the charge transfer band in relation to the locally excited emission decreases from DMABA to DMABMA and DMABEA. In this latter molecule with the weakest acceptor substituent, only a broad shoulder remains of the charge transfer fluorescence. This behavior can be traced back either to a faster formation rate of the charge transfer state or it can be explained by different intrinsic rates for the radiative and nonradiative relaxation processes of the charge transfer species.

In Table 1, the fluorescence quantum yields of DMABA in some selected solvents are listed. The two fluorescence bands of the locally excited and the charge transfer emission are separated by fitting the experimental spectra, rescaled to a wavenumber axes, to the sum of two logarithmic-normal shape functions. This procedure was formulated by Maroncelli and Fleming[20] which was based on the work of Siano and Metzler.[21] An asymmetric emission band is fitted using a set of four

TABLE 1: Fluorescence Quantum Yields of LE and CT Bands and Their Ratio for the Compound DMABA at Room Temperature in Different Solvents

	isopentane	diethyl ether	*n*-butyl chloride	*n*-butyro-nitrile	acetonitrile
polarity Δf	0	0.17	0.21	0.28	0.31
ϕ_f(LE)	0.024	0.036	0.053	0.014	0.002
ϕ_f(CT)	a	0.037	0.049	0.063	0.018
ϕ_f(CT)/ϕ_f(LE)		1.0	0.9	4.4	7.5

[a] No significant charge transfer emission.

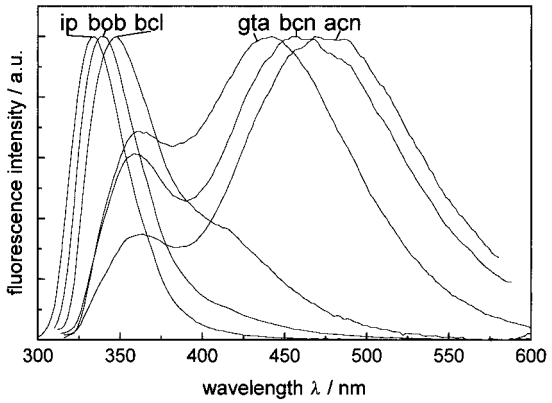

Figure 4. Corrected fluorescence spectra of DMABA in isopentane (ip), dibutyl ether (bob), *n*-butyl chloride (bcl), glycerol triacetate (gta), *n*-butyronitrile (bcn) and acetonitrile (acn) at room temperature normalized to the intensity maximum.

parameters related to the band height, band frequency, the band width, and its asymmetry. The width and asymmetry of the LE band are generally fixed to values measured in isopentane. This was done by using the SPECWORK program.[22]

The fluorescence quantum yields of the alkylated compounds DMABMA and DMABEA are in general 1 order less than those of DMABA. In all three systems, the ratio ϕ_f(CT)/ϕ_f(LE) increases by increasing the solvent polarity as shown for DMABA in Table 1. The charge transfer emission is growing relative to the locally excited fluorescence, a behavior presented in Figure 4 in parallel to the observations for other TICT systems.[2,23]

By recording excitation spectra at different emission wavelengths showing equivalent band shapes at the same position, dependencies of the excitation wavelength on the fluorescence emission spectra could be excluded. Concentration effects could also be excluded in an absorption range between 0.01−1 of the maximum.

As clearly demonstrated in Figure 4, the fluorescence band maxima of the LE and CT emission are a function of the solvent polarity. This solvatochromic red shift indicates that both excited species and especially the charge transfer species possess larger dipole moments than the ground state. By using the eqs 3 and 4 introduced by Lippert and Mataga,[24,25] the excited state dipole moments could be estimated:

$$\frac{\Delta(\hat{\nu}_g - \hat{\nu}_e)}{\Delta(\Delta f)} = \frac{2}{hca^3}(\mu_e - \mu_g)^2 \qquad (3)$$

$$\Delta f = \frac{\epsilon - 1}{2\epsilon + 1} - \frac{n^2 - 1}{2n^2 + 1} \qquad (4)$$

Δf describes the orientational polarization and is used as polarity parameter, $\hat{\nu}_g$ and $\hat{\nu}_e$ are the maxima of absorption and emission bands, μ_e and μ_g the excited and ground state dipole moments, a is the Onsager radius, ϵ is the solvent dielectric constant, and n its refractive index, while h and c have their usual meaning. Equation 3 is based on the following main assumptions: (i) the charge distribution of the molecule is reduced to a point dipole, (ii) the solvent is described by a dielectric continuum, and (iii) the solvent is fully relaxed on the time scale of emission.

TABLE 2: Determination of the Differences between the Excited State and Ground State Dipole Moments ($\mu_e - \mu_g$) of DMABA[a]

	LE emission		CT emission	
	ν_{max}	$<\nu>$	ν_{max}	$<\nu>$
$\Delta\nu/\Delta(\Delta f)$ (cm^{-1})	−8100	−6500	−15 000	−18 300
$(\mu_e - \mu_g)^b$ (Debye)	10 ± 2	9 ± 2	14 ± 2	15 ± 2

[a] From the slopes of a solvatochromic plot including the solvents: isopentane, dibutyl ether, diethyl ether, ethyl acetate, *n*-butyl chloride, *n*-butyronitrile, acetonitrile. The solvatochromic slopes are calculated on the basis of the absolute maximum ν_{max} and on the first moment $<\nu>$ of the emission bands of the LE and CT fluorescence. [b] Setting $a = 5$ Å.

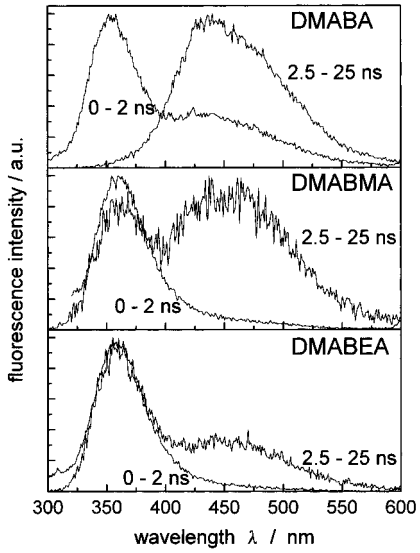

Figure 5. Directly recorded time-resolved fluorescence spectra of the three compounds DMABA, DMABMA, and DMABEA at 153 K in *n*-butyl chloride using an excitation wavelength of $\lambda_{exc} = 300$ nm presenting two time windows (0−2 and 2.5−25 ns), normalized to the maximum fluorescence intensity. The spectra are uncorrected and not deconvoluted from the excitation pulse.

By applying eq 3, it is possible to derive the differences of the dipole moments of the locally excited and the charge transfer emission relative to the ground state from the solvatochromic slopes using an assumption for the Onsager radius a. In agreement with refs 18 and 26, the following estimate is used: $a = 5$ Å. The emission band maxima are characterized by the absolute maximum $\hat{\nu}_{max}$ and the first moment $\langle\nu\rangle$ of the fluorescence band both accessible from the logarithmic-normal fits. Taking into account the error bars of the calculated dipole moments, no significant differences could be observed by using $\hat{\nu}_{max}$ or $\langle\hat{\nu}\rangle$. The slopes and the related dipole moments presented in Table 2 are in the same range as the analogous nitrile and ester compounds.[18,26] The corresponding evaluation of the solvatochromic shift of DMABMA and DMABEA is not reasonable because the long wavelength emission is too weak for a clear determination of the band maxima.

3.2. Time-Resolved Experiments. Figure 5 contains time-resolved fluorescence spectra and illustrates that in the early time window the relative contribution of the long wavelength emission (CT) decreases in the order hydrogen-substituted (DMABA), methyl (DMABMA), and ethyl (DMABEA)-alky-

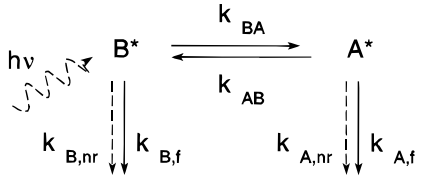

Figure 6. Two-state kinetic scheme assuming that only the state B* can be directly excited and the charge transfer species A* is formed by an adiabatic photoreaction.

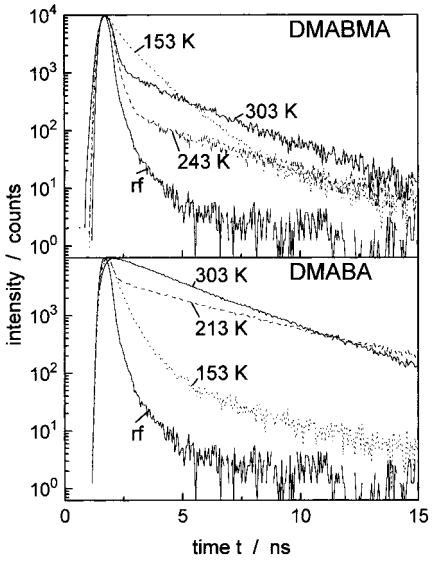

Figure 7. Fluorescence decay traces of DMABMA and DMABA in *n*-butyl chloride at three selected temperatures setting λ_{exc} to 300 nm and λ_{em} to 340 nm. The plots also contain the response function rf from the excitation pulses (BESSY).

lated compounds consistent with the steady-state spectra (Figure 3). In the late time window, only the charge transfer emission is observable for DMABA, while for DMABMA and DMABEA, the evolution favors more and more the locally excited fluorescence band in the spectrum. These observations indicate that the photophysics of amides should be describable by a kinetic model, consisting of two excited species as introduced by the TICT mechanism (Figure 6). There seems to be no hint for the necessity of including a further species. Figure 5 also allows the conclusion that the system undergoes an adiabatic photoreaction because little or no CT band is observed in the early time window. The charge transfer state is therefore populated from the directly excited LE species, although from these experiments alone some direct excitation of the long wavelength emission band can not be totally excluded.

In the following, the fluorescence dynamics will be discussed in more detail, because the kinetic behavior of the investigated compounds is more complex than usual and requires a careful description of the experimental results. To give a better understanding, let us first consider the temperature dependent fluorescence decays, presented in Figure 7, in a more qualitative way in relation to the two-state kinetic model of Figure 6.

In the case of a reversible adiabatic reaction, the so-called high-temperature range,[1,27] the two-state model predicts that a common monoexponential decay should be obtained for both bands after an initial equilibration, which is too fast to be observable here. By lowering the temperature, the backward reaction k_{AB} decreases more rapidly than the formation rate k_{BA}. This induces the appearance of a second shorter time constant measurable only within the short wavelength emission band from which the adiabatic photoreaction rate k_{BA} can be deduced. A further lowering of the temperature implies a growing relative amplitude of this shorter time constant at the cost of the slower decay which vanishes in the low-temperature limit.

The fluorescence decay traces of DMABA and DMABMA in Figure 7, monitored in the LE emission band, are qualititvely in accordance with the above described characteristics and the stationary measurements as well as with the kinetic model in Figure 6.

A similar behavior is also observed in other solvents such as *n*-butyronitrile, ethyl acetate, and diethyl ether. This would imply that the experimental decays fitted to a sum of two exponential functions should be sufficient to reach a satisfactory description over the complete spectral range. If the two-state model holds, the ratio of both preexponential factors should show a value of -1 in the long wavelength range, where the LE band does not contribute.

In Table 3, results of the multiexponential fits of the measured fluorescence decay traces are presented for selected temperatures. The strongly curved traces in Figure 7, even in solvents, such as *n*-butyl chloride, at low temperature and the necessity for triexponential fits even in the nonpolar solvent isopentane (Table 3) document a complex behavior of the fluorescence time evolution in the photophysics of these amides. In contradiction to the kinetic model introduced, three and not two exponential terms are in general necessary to reach a satisfactory fit. Surprisingly, also the emission decays in the nonpolar solvent isopentane are much faster and do not show the expected monoexponential decay as observed for the nitrile derivatives, although in the stationary fluorecence spectra, e.g., Figure 4, no charge transfer band could be seen and there seems to be no deactivation of the locally excited state toward a charge transfer species.

On the other hand, there exists no serious reason to interpret these three exponential terms with three distinct species. It seems to be more reasonable to assume a nonradiative deactivation channel inducing a distribution of time constants. This hypothesis is in agreement with the deviation of the investigated compounds from a monoexponential decay in isopentane (Table 3). The assumption of a distributed nonemissive deactivation rate is supported by the fluorescence experiments at 77 K in *n*-butyl chloride. At this temperature, the charge transfer formation is stopped, but again two exponential terms instead of one are necessary to fit the time-resolved decay. The mean time constant is significantly shorter than that for the nitrile DMABN measured under the same conditions (around 5 ns).[28] On this basis, the adjusted parameters for the experiments in *n*-butyl chloride, presented at two selected temperatures in Table 3, become understandable. It has to be emphasized that these data are nevertheless in rough accordance with the simple two-state kinetic model (Figure 6), but they show a more complex dynamics related to a distributed deactivation channel k_B.

Focusing on the mean decay time constants at 340 nm and 153 K of the three investigated compounds, an increase from DMABA to DMABMA and to DMABEA is reported consistent with a decrease of the charge transfer formation rate constant k_{BA}, in parallel with the conclusion from the stationary fluorescence spectra in Figure 3.

In Table 3, the results of a global analysis of the ethyl-substituted compound DMABEA at 153 K in *n*-butyl chloride are presented and the fits measured in the high and low energy edge of the dual fluorescence spectrum are shown in Figure 8. The sum of the two negative preexponential factors in the long wavelength region of the emission spectrum corresponding to rise times and the preexponential factor of the decay time add up to zero, typical for the two-state kinetic scheme. The rise of the long wavelength band is thus characterized by the same nonexponential behavior as that of the decay observed in the

TABLE 3: Multiexponential Fit Parameters for Selected Fluorescence Decay Traces of the Three Investigated Compounds in Isopentane and *n*-Butyl Chloride, Including the Quality Parameter χ^2 and Durbin−Watson

system	solvent	λ_{exc}/nm	λ_{em}/ nm	temp/K	τ_1/ns (α_1)	τ_2/ns (α_2)	τ_3/ns (α_3)	$\langle\tau\rangle$/ns[a]	χ^2	Durbin-Watson
DMABA	isopentane	300	350	155	0.19 (0.75)	0.81 (0.24)	3.64 (0.01)	0.38	1.22	1.92
DMABMA		300	350	155	0.11 (0.93)	0.46 (0.072)	1.90 (0.003)	0.14	1.30	2.00
DMABA	*n*-butyl chloride	300	340	303	1.73 (0.29)	3.06 (0.71)		2.67	1.18	1.79
		300	340	153	0.11 (0.91)	2.14 (0.074)	12.3 (0.014)	0.26[b]	1.22	1.84
		300	500	153	1.06 (0.39)	3.64 (0.56)	9.79 (0.06)	2.98	1.02	1.81
		300	340	77	1.32 (0.88)	2.91 (0.12)		1.51	1.13	1.96
DMABMA		280	340	303	<0.1 (0.99)	2.62 (0.01)		<0.1	1.19	1.81
		280	340	153	0.18 (0.65)	0.84 (0.35)	4.12 (0.006)	0.43	1.12[c]	
		280	500	153	0.18 (−0.55)	0.84 (−0.45)	4.12 (1)	4.12		
		280	340	77	0.93 (0.59)	1.96 (0.41)		1.35	1.18	1.85
DMABEA		275	340	153	0.31 (0.59)	1.44 (0.41)	4.07 (0.01)	0.80	1.12[d]	
		275	520	153	0.31 (−0.75)	1.44 (−0.25)	4.07 (1)	4.07		

[a] Rise times are neglected. [b] Excluding the long decay component. [c] Results of a global analysis by linking the three time constants including decays for λ_{em} equal to 340, 400, 450, and 500 nm. [d] Results of a global analysis by linking the three time constants including decays for λ_{em} equal to 340, 370, 400, 430, 460, 490, and 520 nm.

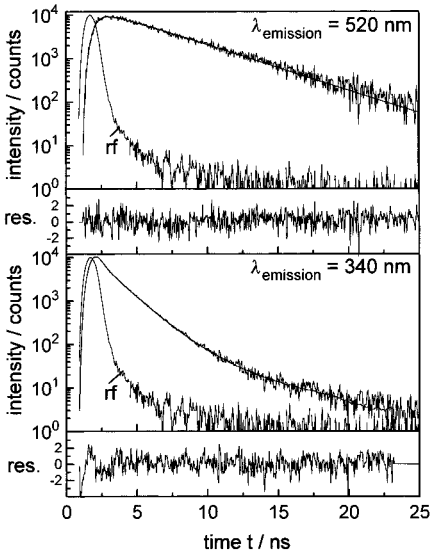

Figure 8. Results of a global analysis of the experiment DMABEA in *n*-butyl chloride at 153 K excited at $\lambda_{ex} = 275$ nm and monitored at λ_{em} equal to 340, 370, 400, 430, 460, 490, and 520 nm. The fluorescence decay curves at $\lambda_{em} = 340$ and 520 nm are presented including the model function, the excitation pulse, and the residuals.

LE band. For DMABMA, this kind of kinetics is also observed (Table 3). This evidences that the charge transfer species is completely populated from the directly excited LE precursor for the alkylated molecules, as could already be supposed from Figure 5. In the analogous measurements of DMABA, such rise times could not be demonstrated probably due to the limited experimental time resolution.

4. Discussion

Summarizing the above observations, it has to be concluded that the well-known TICT mechanism and the related two-state kinetic scheme with discrete rate constants (Figure 6) are not sufficient to understand the complete data set of the amide derivatives presented here. Two main extensions summarized in Figure 9 can be suggested to generate a more consistent model. (i) Firstly, a strongly inhomogeneous ground state related to the multiple torsional degrees of freedom may be responsible for the distributed rate constants. The torsions possible within the amide function are indicated in Figure 9. Different conformers may correspond to different acceptor strengths of this group. This large variety of conformations can lead to slightly different TICT formation kinetics thus complicating the fluorescence decay traces.

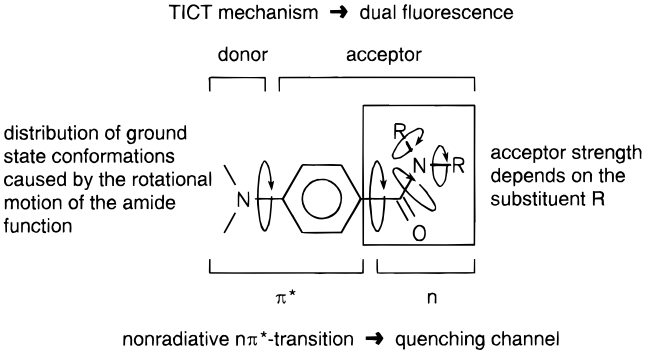

Figure 9. Scheme to summarize the controlling factors of the dynamics of the investigated compounds.

(ii) Secondly, the energetically low-lying $n\pi^*$-transition of the amide function can be the source of the additional nonradiative deactivation cannel, also observed in alkane solvents. A similar effect has already been postulated for derivatives of DMABN, where the nitrile group is replaced by aldehyde or keto groups.[29,30] The ability of the amide function to accept electrons can be controlled by the inductive effect of different alkyl substituents.

It is reasonable to assume that in the alkylated compounds DMABMA and DMABEA the steric influence of the methyl or ethyl groups is stronger than in DMABA. This suggests a more planar conformation for DMABA compared to the alkylated molecules. Molecular mechanics and AM1 calculations lead to values of the torsional angle, measured between the plane of the aromatic ring and the amide functional group, respectively, of 51° to 74° for representatives of substituted *N*,*N*-dimethyl benzamides, while a value of 28° has been determined for benzamides. More planarity for benzamides is also indicated by natural abundance ^{17}O spectroscopic data which have been correlated with Hammet σ^+ constants, and the ρ^+ value of ∼2 for alkylated benzamides is small compared to a value of 6.7 reported for benzamides.[31] The decreasing relative intensity of the charge transfer band from DMABA to DMABMA and to DMABEA and the decreasing rate of the TICT formation can be simply explained by the inductive effect of different substituents on the amide function diminishing the acceptor ability, but also by their steric crowding which diminishes resonance interactions as a result of poorer orbital overlap. The fact that the fluorescence quantum yields of the alkylated compounds are one order of magnitude smaller than for DMABA (Table 1) correlates with a higher efficiency of the $n\pi^*$-quenching channel supported by the faster kinetics of DMABMA as compared to DMABA in isopentane (Table 3).

The strongly nonexponential decays in the glassy state at 77 K (Table 3) are a further hint for the $n\pi^*$-character of the deactivation channel, because for these conditions, large conformational changes are not possible. The ground state torsional distribution inducing conformation-dependent $n\pi^*$ deactivation rates can thus be responsible for the deviation from monoexponential kinetics observed for all experimental conditions used.

In spite of the additional complexity of the photophysics of the amides and their low fluorescence quantum yields, these compounds may be useful for developing fluorescence probes[32] by coupling a crown ether function to the amino group on the amide substituent. This crown ether function can bind metal cations in solution, and this can be used to quantify their level for analytical purposes or to follow the time and spatial evolution of concentration gradients in biological samples. Recently, a dual fluorescent crown ether derivative of DMABN was presented which strongly binds to Ca^{2+}-ions whereby the long wavelenth A-band is diminished.[23] Using this approach for the amide derivatives described here, it can be predicted that the Ca^{2+} adduct should show an enhanced A-band because the metal cation will increase the acceptor strength of the amide substituent. First results confirming this prediction have been obtained.[33]

Acknowledgment. The authors gratefully acknowledge support of this work by the Deutsche Forschungsgemeinschaft (SFB 337) and by the BMFT (Project 05414 FAB1).

References and Notes

(1) Grabowski, Z. R.; Rotkiewicz, K; Siemiarczuk, A.; Cowley, D. J.; Baumann, W. *Nouv. J. Chim.* **1979**, *3*, 443.

(2) Rettig, W. *Angew. Chem., Int. Ed. Engl.* **1986**, *25*, 971.

(3) Rettig, W. In *Topics in Current Chemistry*; Mattay, J., Ed.; Springer Verlag: Berlin, 1994; Vol. 169, p 253.

(4) Schuddeboom, W.; Jonker S. A.; Warman, J. M.; Leinhos, U.; Kühnle, W.; Zachariasse, K. A. *J. Phys. Chem.* **1992**, *96*, 10809.

(5) von der Haar, T.; Hebecker, A.; Il'ichev, Y.; Jiang Y.-B.; Kühnle, W.; Zachariasse, K. A. *Recl. Trav. Chim. Pays-Bas* **1995**, *114*, 430.

(6) Weisenborn, P. C. M.; Huizer, A. H.; Varma, C. A. G. O. *Chem. Phys.* **1988**, *126*, 425.

(7) Wermuth, G.; Rettig, W.; Lippert E. *Ber. Bunsen-Ges. Phys. Chem.* **1981**, *85*, 64.

(8) Rettig, W.; Wermuth, G. *J. Photochem.* **1985**, *28*, 351.

(9) Dedonder-Lardeux, C.; Jouvet, C.; Martrenchard, S.; Solgadi, D.; McCombie, J.; Howells, B. D.; Palmer, T. F.; Subaric-Leitis, A.; Monte, C.; Rettig, W.; Zimmermann, P. *Chem. Phys.* **1995**, *191*, 271.

(10) Rettig, W.; Dedonder-Lardeux, C.; Jouvet, C.; Martrenchard-Barra, S.; Szrifiger, P.; Krim, L.; Castano, F. *J. Chim. Phys. (France)* **1995**, *92*, 465.

(11) Rotkiewicz, K.; Rettig, W. *J. Lumin.* **1992**, *54*, 221.

(12) Field, L.; Hughmark, P. B.; Shumaker S. H.; Marshall, W. S. *J. Am. Chem. Soc.* **1961**, *83*, 1983.

(13) Coppinger, G. M. *J. Am. Chem. Soc.* **1954**, *76*, 1372.

(14) Vogel, M.; Rettig, W. *Ber. Bunsen-Ges. Phys. Chem.* **1987**, *91*, 1241.

(15) Rettig, W.; Vogel, M.; Klock, A. *EPA Newsl.* **1986**, *27*, 41.

(16) Connor, D. V.; Phillips, D. *Time Correlated Single Photon Counting*; Academic Press: London, 1984.

(17) *Globals Unlimited*, Revision 3; Laboratory for Fluorescence Dynamics, University of Illinois: Urbana, IL, 1992.

(18) Rettig, W.; Braun, D.; Suppan, P.; Vauthey, E.; Rotkiewicz, K.; Luboradzki, R.; Suwinska, K. *J. Phys. Chem.* **1993**, *97*, 13500.

(19) Revill, J. A. T.; Brown, R. G. *Chem. Phys. Letters* **1992**, *188*, 433.

(20) Maroncelli, M.; Fleming, G. R. *J. Chem. Phys.* **1987**, *86*, 6221.

(21) Siano, D. B.; Metzler, D. E. *J. Chem. Phys.* **1969**, *51*, 1856.

(22) Schwarzburg, K. *Specwork Programm*; Version 3.1.; Berlin, 1993.

(23) Létard, J.-F.; Delmond, S.; Lapouyade, R.; Braun, D.; Rettig, W.; Kreissler, M. *Recl. Trav. Chim. Pays-Bas* **1995**, *114*, 517.

(24) Lippert, E. *Z. Elektrochem.* **1957**, *61*, 962.

(25) Mataga, N.; Kaifu, Y.; Koizumi, M. *Bull. Chem. Soc. Jpn.* **1956,** *29*, 465.

(26) Baumann, W.; Bischof, H.; Fröhling, J.-C.; Brittinger, C.; Rettig, W.; Rotkiewicz, K. *J. Photochem.* **1992**, *64*, 49.

(27) Rettig, W.; Lippert, E. *J. Mol. Struct.* **1980**, *61*, 17.

(28) Rettig, W.; Vogel, M.; Lippert, E.; Otto, H. *Chem. Phys.* **1986**, *103*, 381.

(29) Dähne, S.; Freyer, W.; Teuchner, K.; Dobkowski J.; Grabowski, Z. R. *J. Lumin.* **1980**, *22*, 37.

(30) Dobkowski, J.; Kirkor-Kaminski, E.; Koput, J.; Grabowski, Z. R. *J. Lumin.* **1982**, *27*, 339.

(31) Spychala, J.; Boykin, D. W. *J. Chem. Res. Synops.* **1993**, 426.

(32) Rettig, W.; Lapouyade, R. In *Topics in Fluorescence Spectroscopy*; Lakowicz, J. R., Ed.; Plenum Press: New York, 1994; Vol. 4, p 109.

(33) Delmond, S.; Létard, J.-F.; Lapouyade, R. *NATO ASI Series*, Bordeaux, 1996.